African Journal of Advanced Pure and Applied Sciences (AJAPAS)
Online ISSN: 2957-644X
Volume 5, Issue 1, 2026
Page No: 205-212
Website: https://aaasjournals.com/index.php/ajapas/index
ISI 2025: 1.126 **SJIFactor 2024: 6.752** **معامل التأثير العربي: 1.62**

Thermal Analysis of Medium Voltage Single Core Armoured XLPE Cable

Mohamed A Alsharif [1 *], Khlid Ben Hamad [2], Abdulgader Alsharif [3], Mohamed Salem [4]
[1] Department of communication and information technology, Technical College of Civil Aviation and Meteorology, Espia, Libya
[2] Department of Electrical and Electronic Engineering, Faculty of Engineering Fezzan, University Fezzan, Libya
[3] Department of Electric and Electronic Engineering, College of Technical Sciences, Sebha, Libya
[4] Libyan Authority for Scientific Research, Tripoli, Libya

التحليل الحراري لكابل أرضي ذو جهدٍ متوسطٍ أحاديّ النواة مدرع ومعزول بالبولي إيثيلين المتشابك

محمد ابوبكر الشريف [1*]،خالد بن حماد [2]، عبدالقادر الشريف [3] ، محمد سالم [4]
[1] قسم هندسة الاتصالات وتقنية معلومات الطيران، كلية تقنية الطيران المدني والأرصاد الجوية، اسبيعة، ليبيا
[2] قسم الهندسة الكهربائية والالكترونية، كلية الهندسة، جامعة فزان، الرقيبة، ليبيا
[3] قسم الهندسة الكهربائية و الالكترونية، كلية العلوم التقنية، سبها، ليبيا
[4] الهيئة الليبية للبحث العلمي، طرابلس، ليبيا

[*]Corresponding author: moh.alsharif@sebhau.edu.ly

Received: November 14, 2025	Accepted: January 22, 2026	Published: February 05, 2026

Abstract:
Worldwide, electricity distribution networks primarily rely on medium-voltage cross-linked polyethylene underground cables. The thermal performance of these cables is critical to their operational stability and service lifespan, with operating temperature and thermal history being the key influencing factors. This paper presents an accurate thermal model for a buried single-core armoured cross-linked polyethylene medium-voltage cable system, developed using the finite element method. Key parameters, such as ampacity, cable construction, installation configuration, the thermal characteristics of the surrounding soil, and the prevailing ambient temperature, are considered. The thermal field response under both steady-load and realistic time-varying load conditions, including daily load variations, is investigated. Electrical losses are calculated and integrated into the thermal analysis. The simulation results reveal significant time-dependent temperature gradients and cyclic thermal variations within the cable, highlighting the necessity of transient thermal analysis. This study contributes to a deeper understanding of the modelling and analysis of thermal behaviour of buried armoured cross-linked polyethylene cables, enabling improved assessment of plant integrity and the extension of service life.

Keywords*:* XLPE medium-voltage cables, Thermal behaviour, Finite element method, Time-dependent temperature gradients, Electrical losses.

الملخص
عالميًا، تعتمد شبكات التوزيع الكهربائية بشكل أساسي على الكابلات الأرضية ذات الجهد الكهربائي المتوسط المصنوعة من البولي إيثيلين المتشابك. يُعد الأداء الحراري لهذه الكابلات عاملًا مهمًا لاستقرارها التشغيلي وطول عمرها الافتراضي، حيث يُعتبر كل من درجة حرارة التشغيل والتاريخ الحراري من أهم العوامل المؤثرة. تقدّم هذه الورقة نموذجًا حراريًا دقيقًا لنظام كابل مدفون أحادي القلب ومُدرَّع من نوع البولي إيثيلين المتشابك للجهد الكهربائي المتوسط، تم تطويره باستخدام طريقة العناصر المحددة، مع الأخذ في الاعتبار معايير رئيسية مثل سعة التيار الكهربائي، وبنية الكابل، وطريقة التركيب، والخصائص الحرارية للتربة، ودرجة الحرارة المحيطة. تم دراسة الاستجابة الحرارية للكابل تحت كل من ظروف الحمل الثابت والحمل المتغير مع الزمن، مع مراعاة التغيرات اليومية في الحمل، وتم حساب المفاقيد الكهربائية وإدماجها ضمن التحليل الحراري. تُظهر نتائج المحاكاة وجود تدرجات حرارية واضحة تعتمد على الزمن وتغيرات دورية للحرارة داخل

الكابل، مما يبرز ضرورة إجراء التحليل الحراري العابر. تُسهم هذه الدراسة في فهم أعمق لنمذجة وتحليل السلوك الحراري للكابلات المدفونة والمدرعة من نوع البولي إيثيلين المتشابك، بما يُتيح تقييمًا أفضل لسلامة النظام وإطالة عمر الخدمة.

الكلمات المفتاحية: كوابل البولي إيثيلين المتشابك ذات الجهد الكهربائي المتوسط، طريقة العناصر المحددة، التدرج الحراري مع الزمن، المفاقيد الحرارية.

Introduction

Medium-voltage distribution networks typically use underground cables to carry several hundred amperes at operating voltages between 11kV and 33 kV [1, 2]. Cross-Linked Polyethylene (XLPE) insulated MV underground cables have been widely used in power transmission and distribution networks since the 1980s due to their excellent electrical, thermal, and mechanical properties [3, 4]. These cables provide reliable service, but over time, the aging of solid insulating materials and systems adversely affects their performance, ultimately reducing their service life [5]. In addition, the XLPE cable conductor operating temperature should not exceed 90 °C to avoid structural changes in the dielectric material that could shorten its operational lifespan [6]. Furthermore, the aging of underground cables depends on their operating temperature; as the temperature increases, the lifespan of these cables decreases, and vice versa [7].

During the online operation of a single-phase cable, the current varies as the load changes. These load cycles cause the cable to repeatedly heat up and cool down during system operation. This temperature change is due to the heat dissipated in the conductor, which increases with the amount of current transmitted. The cable heats up under high load and cools down under low load. As the temperature rises, the cable materials expand; conversely, a drop in temperature causes them to contract. These temperature variations lead to changes in the size of cable components resulting in mechanical strain.

Thermal expansion caused by thermal cycling induces physical changes in the cable. Since the cable is either installed in fixed ducts or directly buried in the ground, it is constrained from expanding or moving freely. The difference in thermal expansion coefficients between the cable's components such as the conductor, insulation, and armour leads to internal stress. For example, the thermal expansion coefficient of XLPE is about 20 times higher than that of the copper conductor, causing the outer layer of the insulation to cool faster than its conductor. This results in uneven crystallite formation within the insulation, altering the cable structure in the longitudinal, radial, and transverse directions. The expansion of the insulation also exerts pressure on the conductor, weakening the copper and potentially damaging the insulation, thereby degrading the cable's structural integrity [8]. Consequently, the temperature of the cable insulation may exceed its rated limits, accelerating the degradation of insulation materials and increasing the likelihood of cable failure.

Temperature is the most significant factor influencing cable insulation and consequently its degradation [9]. It was found that temperature, which is influenced by the load, is the main factor leading to cable failures during operation in power systems [10]. Most medium-voltage underground cable faults are attributed to overheating, particularly due to the Joule effect, which significantly affects failure rates in electrical cables, joints, and other components [11–15]. Heat generation in medium-voltage underground cables is affected by changes in ambient conditions, including the temperature and thermal resistivity of the surrounding soil, which influence the cable's ability to dissipate heat and maintain safe operating temperatures [16, 17].

By monitoring the actual cable temperature, it is possible to evaluate the thermal impact of daily load variations and take appropriate action [18]. This allows an accurate estimation of the thermal lifetime of the cable, supporting effective maintenance and replacement planning [19, 20]. Although the thermal performance of underground cables has been studied over the last decades, deeper knowledge is still required to address their management challenges in modern infrastructure.[21]. Measuring the temperature of cables while they are in operation is highly challenging [22]. Furthermore, optimizing the current-carrying capacity of underground cables in real time, based on temperature and load variations, remains a difficult task due to practical and technical limitations [18]. In particular, the thermal characteristics of underground cables have not been fully characterized [23]

This paper investigates the thermal behaviour of a medium-voltage XLPE cable under service conditions. An accurate thermal model of a buried 11 kV single-armoured XLPE cable is developed using the finite element method in COMSOL Multiphysics. Cable operating temperature is estimated. Furthermore, the thermal response of a typical XLPE cable is analysed, taking into account the ambient conditions of the given installation. The model system is based on a single-armoured XLPE cable, with dimensions and characteristics derived from previous studies, as shown in Figure 1 [3]. The conductor is made of copper with a cross-sectional area of 95 mm², and the overall diameter of the cable is 20.5 mm.

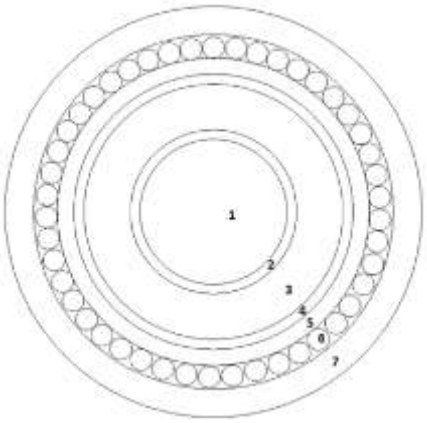

Figure 1: Standard configuration of a single-core 95 mm² XLPE cable: (1) copper conductor, (2) semiconductive layer, (3) cross-linked polyethylene insulation, (4) semiconductive insulation, (5) bedding layer, (6) aluminum wire armour, and (7) polyvinyl chloride outer sheath [3].

Material and methods

Thermal Model

Finite element simulations of the cable's thermal performance were conducted under both steady-load and time-varying conditions, incorporating time-series data to account for daily load variations. These simulations evaluate the cable's thermal response over a 24-hour period, reflecting the fact that the thermal response time of buried cables often spans a full day. Several parameters influence the thermal behavior of an installed cable system, including the specified ampacity, the cable design, installation conditions, the ambient temperature, and the thermal characteristics of the surrounding soil. Heat transfer to the environment is influenced by the structure and material properties of the conductor, its insulation, armor, and sheath, as well as the surrounding trench-fill material and ambient environmental conditions [24].

Representing the designated heat dissipation region, the two-dimensional domain consists of a cable cross-section embedded within a semicircular region of surrounding soil and trench fill with a diameter of 6 meters. The cable model is represented as buried in a 0.6-meter by 0.6-meter square trench filled with sand, with its centre located 0.3 meters beneath the soil surface and the trench surface aligned with the surrounding ground.

The primary heat source is the Joule effect in the conductor, calculated as the conductor's resistance (in ohms, **Ω**) multiplied by the square of the current (in amperes, A) passing through it, expressed as I^2R. The model uses one-day load profiles as input, and its output reflects the cable's thermal response under the specified installation and environmental settings.

To derive the heat transfer partial differential equation (PDE), the following equations and physical principles are introduced; The fundamental equation of energy conservation in transient heat conduction, which depends on time, is given by:

$$\rho C_p \frac{\partial T}{\partial t} + \nabla \cdot q = 0 \tag{1}$$

Here, ρ represents the density (kg/m³), C_p is the specific heat capacity (J/(kg·K)), T is the temperature (K), t is the time (s), and q is the heat flux vector (W/m²). The heat transfer through a material is described by Fourier's law:

$$q = -K\nabla T \tag{2}$$

Here, K represents the thermal conductivity, expressed in W/(m·K),

Next, Fourier's law is substituted into the conservation equation, and the heat generation source term, Q, is added to the right-hand side to represent heat transfer. The resulting equation is:

$$\rho C_p \frac{\partial T}{\partial t} = \nabla \cdot [K\nabla T] + Q \tag{3}$$

Where Q is a heat source (W/m³).

Since the cable length is much greater than its size, end effects are neglected, and the heat transfer is analysed in two dimensions [25]. Equation (3) is addressed by solving the two-dimensional domain described in Equation 4.

$$\rho C_p \frac{\partial T}{\partial t} = \frac{\partial}{\partial x}\left[K \frac{\partial T}{\partial x}\right] + \frac{\partial}{\partial y}\left[K \frac{\partial T}{\partial y}\right] + Q \quad (4)$$

Equation 4 solves the temperature at any point based on given thermal conductivity and heat generation overall cable medium. In addition, equation 4 is used to solve the power cable thermal circuit considering the conditions at the boundaries.

Boundary conditions:
Thermal boundary conditions are applied at two principal thermal interfaces: (a) the soil surface and (b) a semicircular boundary extending into the native soil.

Both boundaries are set to 288 K (15 °C), as described in [26]. The thermal conductivity is taken as 0.833 W/(m·K) for the native soil, 0.2 W/(m·K) for the sand backfill, and 0.38 W/(m·K) for the XLPE cable insulation.

Heat flux continuity is set across the internal boundaries between the different cable materials, as follows:

$$n \cdot (q_1 - q_2) = 0 \quad (5)$$

Where: q_1 (W/m²) is the inward heat flux and q_2 (W/m²) is the outward heat flux. The initial temperature field was set uniformly to: T (t_o) = 288 K (15□C).

Heat Loss Representation:

The heat generation source term is included in the model and represents the Joule losses resulting from current flow in the conductor (Q_c). The heat source is calculated from the conductor's total power loss per unit cross-sectional area. Accordingly, the expression for $Q_c$is [27]:

$$Q_c = \frac{I^2 \cdot R}{A_c} \quad (6)$$

Here, the current through the conductor (I), the cross-section area of the conductor (A_c), and the alternating current resistance (R) of the conductor at its peak operating temperature are expressed as:

$$R = R_{dc}\,(1 + y_s + y_p) \quad (7)$$

Here, the direct current resistance of the conductor (R_{dc}) at the peak operating temperature, the proximity effect factor (y_p) is neglected because the cable is a single-phase type with non-magnetic aluminum wire armour [28], and the skin-effect factor (y_s) is given by:

$$y_s = \frac{x_s^4}{192 + 0.8 \cdot x_s^4} \quad (8)$$

Where, $X_s$is the skin-effect argument, calculated as:

$$x_s^2 = \frac{4 \cdot \omega \cdot k_s \cdot 10^{-7}}{R_{dc}} \quad (9)$$

here, ω is Angular frequency and k_s is the coefficient of skin effect.

Heat dissipation to the environment is controlled by the cable's geometry and the thermal characteristics of the conductor, insulation, armour, sheath, trench-fill material, and surrounding conditions.

Results and discussion
Response to a steady Load
The thermal field of a single buried XLPE cable system is predicted based on the applied load conditions. When a 100-A load step is applied at time zero under an ambient temperature of 288 K, the resulting thermal response is evaluated. The temperature is predicted under a steady load current of 100 A over a 24-hour period. As shown in Figure 2, the curves illustrate the temperature at three measurement points: the conductor (upper curve), the armour (middle curve), and the outer sheath (lower curve).

The system demonstrates fast, medium, and slow dynamic responses: the fast response reflects the rapid heating of the cable itself (i.e., the conductor), the medium response corresponds to the warming of the surrounding insulation (i.e., the armour), and the slow response represents the gradual temperature increase of the trench-fill material surrounding the cable (i.e., the outer sheath).

The steady-state temperature differences between the cable elements have been established as follows: between the conductor and the armour, approximately 1.41 K; between the armour and the outer sheath, approximately 1.16 K; and between the conductor and the outer sheath, approximately 2.57 K. This is explained by the thermal resistances of each cable component being constant; the temperatures across the components remain proportional to their resistances, causing the temperature separation between the core, armour, and sheath to appear constant. By the end of the 24-hour period, the temperatures of the conductor, armour, and outer sheath had stabilized, indicating that the system was nearly at thermal equilibrium due to the balance between heat generated in the conductor and heat dissipated through the insulation, armour, sheath, and surrounding soil.

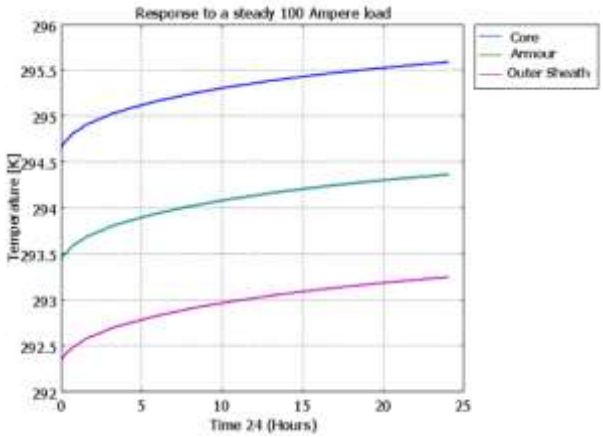

Figure 2: The thermal responses of the conductor, armour, and outer sheath of the XLPE cable subjected to a static load.

Response to load variation

The thermal field response of a single XLPE cable system to load variation was assessed over a 24-hour period. The simulation utilized time-series data representing a real daily load profile [29]. The operational temperature of the cable changed in accordance with daily load variations, exhibiting a total temperature swing of 4.55 K. The system was initially in thermal steady state with a uniform background temperature of 288 K. The cable temperature reached a maximum of 295 K in the conductor at 20:45 and a minimum of 289.5 K in the outer sheath at 04:30, reflecting the different thermal characteristics of the cable components.

The temperature differences between the cable components varied over time: between the conductor and the aluminium wire armour, 0.33–1.76 K; between the armour and the outer sheath, 0.44–2 K; and between the conductor and the outer sheath, 0.77–3.28 K. This variation occurs even though the thermal resistance remains constant and is due to the different dynamic responses of the cable components and the varying load. Figure 3 illustrates the temperature variation across the cable cross-section over the 24-hour simulation, and the corresponding input load current data are shown in Figure 4 [29].

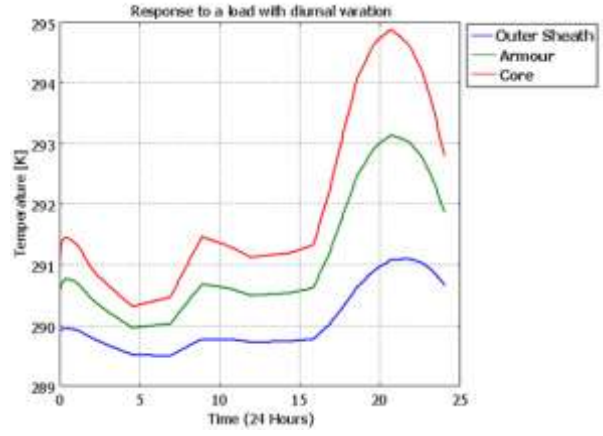

Figure 3: Thermal response of the conductor, armour, and outer sheath of the XLPE cable under the daily load cycle.

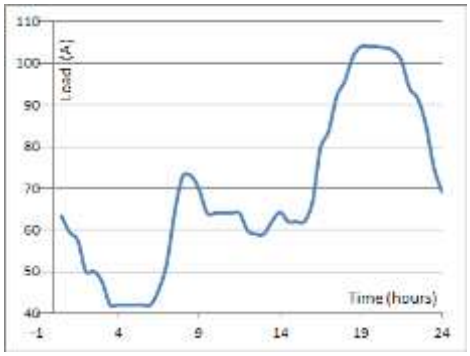

Figure 4: Input load current for the XLPE cable over 24 hours [29].

Figures 5 and 6 illustrate the temperature distribution across the cable cross-section at the point of maximum temperature during a 24-hour analysis. The temperature is consistent over the conductor surfaces due to copper's high thermal conductivity and the consideration of homogeneous internal heat generation. A distinct trefoil pattern is observed in the temperature distribution within the insulation layer, which marks the position of the cable conductor. This pattern reflects the thermal conductivity of the insulation material, with lower temperature values in the surrounding insulation compared to the conductor.

The maximum temperature occurs at the center of the cable and its adjacent areas, with both the magnitude and location of the maximum temperature being consistent. The temperature decreases significantly once the sheath is reached, and the temperature gradient shifts accordingly. Additionally, there is a sharp drop in temperature from 294.879 K at the cable center to 288.15 K, the ambient temperature, in the surrounding soil. The temperature distribution across the cross-section of a buried XLPE cable is relatively uniform around the cable components. The highest temperatures are concentrated near the conductor, gradually decreasing with distance from the conductor. The temperature gradient is most pronounced in areas with higher power losses and diminishes in regions with lower or negligible losses.

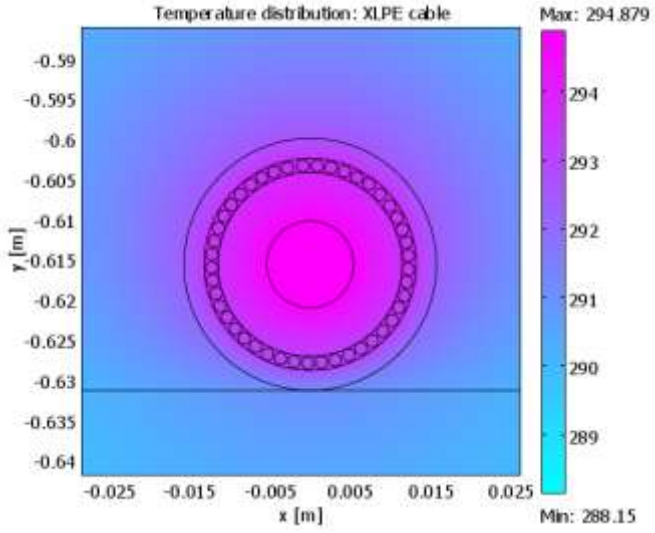

Figure 5: Cross-section of the buried, armoured underground XLPE cable system showing the temperature variation at the point of maximum operating temperature during a 24-hour simulation. The scale on the right-hand side indicates the temperature in Kelvin (K), represented by a pink gradient.

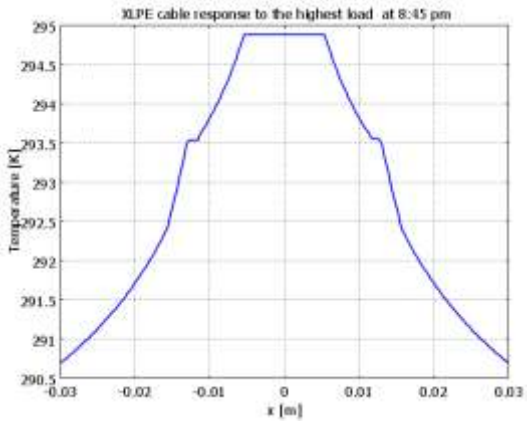

Figure 6: Thermal behaviour along the x-axis XLPE cable system when the temperature reaches its maximum over a 24-hour period. The blue line represents the thermal variation at 20:45 along the same cross-section. Note that the centre of the cable is located at x = 0 m.

The results demonstrate the total thermal losses in the XLPE cable. Heat is conducted from the conductor to the surrounding soil through the cable materials. The temperature rise in the buried cables was predicted considering the 50 Hz power frequency, electrostatic effects, diurnal load variations, and the thermal conductivities of the materials. The highest temperature occurred at the conductor surface and the lowest at the outer sheath, with the temperature difference between the conductor and the surrounding soil also quantified.

Conclusion

An accurate thermal model of a buried armoured XLPE underground cable system under service conditions was developed using the finite element method. The thermal behavior of a medium-voltage cable under both static and variable load conditions over a 24-hour period was analysed. The relationship between the daily load current and cable temperature was predicted. Temperature profiles inside the cable, through the thermal backfill, and extending into the surrounding soil were calculated, and the corresponding thermal conductivities were evaluated. A pronounced gradient in temperature was observed in the cable and changed over time. A methodology for characterizing the thermal performance of medium-voltage cables was introduced, and the system's response to diurnal load variations was assessed.

Compliance with ethical standards

Disclosure of conflict of interest

The authors declare that they have no conflict of interest.

References

[1] P.A. Wallace, M. Alsharif, D.M. Hepburn, and C. Zhou, Failure modes of underground MV cables: Electrical and thermal modelling, in Excerpt from the Proceedings of the COMSOL Conference, 2009.

[2] BS 7870, Specification for distribution cables with extruded insulation of rated voltages of 11 kV to 33 kV Single-core 11 kV to 33 kV cables, British Standards Institution, London, 2016.

[3] M. Alsharif, P.A. Wallace, D.M. Hepburn, and C. Zhou, FEM modelling of electric field and potential distributions of MV XLPE cables containing void defect, in Excerpt from the Proceedings of the COMSOL Conference, Milan, Oct. 2012.

[4] X. Wang, A. Liang, Y. Wang, W. Zhu, Y. Zhao, X. Dai, X. Fan, Y. Xie, and G. Liu, Influence on aggregation structure changes of retired cross-linked polyethylene (XLPE) cable insulation under pre-qualification test, IOP Conference Series: Materials Science and Engineering, vol. 585, p. 012049, 2019.

[5] IEEE Std 1064-1991, IEEE Guide for Multifactor Stress Functional Testing of Electrical Insulation Systems, IEEE, 1991.

[6] S. Tagzirt, D. Bouguedad, A. Mekhaldi, and I. Fofana, Temperature distribution in a 245 kV AC XLPE cable, IEEE Conference on Electrical Insulation and Dielectric Phenomena (CEIDP), 2020, pp. 483–486.

[7] A.S. Alghamdi and R.K. Desuqi, A study of expected lifetime of XLPE insulation cables working at elevated temperatures by applying accelerated thermal ageing, Heliyon, vol. 6, no. 1, 2020.

[8] R. Bartnikas and K. Srivastava, Power and Communication Cables: Theory and Applications, 1st ed. New York, NY, USA: Wiley-IEEE Press, 2003.

[9] E. Inga, P. Sanango, and F. Quizhpi, Determination of the degradation equation for medium voltage XLPE cable at 22 kV, 7th Global Power, Energy and Communication Conference (GPECOM), 2025, pp. 367-371.

[10] M. Qatan, M.E. Farrag, B. Alkali, and C. Zhou, Modeling and analysis of the remaining useful life of MV XLPE cable: Case study of Oman oil and gas power grid, 53rd International Universities Power Engineering Conference (UPEC), 2018, pp. 1–6.
[11] L. Calcara et al., Faults evaluation of MV underground cable joints, AEIT International Annual Conference (AEIT), Florence, Italy, 2019, pp. 1–6.
[12] A. Sturchio, G. Fioriti, M. Pompili, and B. Cauzillo, Failure rates reduction in SmartGrid MV underground distribution cables: Influence of temperature, AEIT Annual Conference - From Research to Industry: The Need for a More Effective Technology Transfer (AEIT), Trieste, Italy, 2014, pp. 1–6.
[13] A. Sturchio, G. Fioriti, V. Salusest, L. Calcara, and M. Pompili, Thermal behavior of distribution MV underground cables, AEIT International Annual Conference (AEIT), Oct. 2015, pp. 1–5.
[14] L. Calcara, M. Pompili, and B.A. Cauzillo, Ampacity of MV underground cables: The influence of soil thermal resistivity, 5th International Youth Conference on Energy (IYCE), May 2015, pp. 1–5.
[15] L. Calcara, S. Sangiovanni, and M. Pompili, MV underground cables: Effects of soil thermal resistivity on anomalous working temperatures, AEIT International Annual Conference, Sept. 2017, pp. 1–5.
[16] M. Olschewski, P. Schäfer, and W. Hill, Continuous safeguarding of rating accuracy, CIRED, vol. 24, no. 1, pp. 83–86, 2017.
[17] P. Ocłoń, The effect of soil thermal conductivity and cable ampacity on the thermal performance and material costs of underground transmission line, Energy, vol. 231, p. 120803, 2021.
[18] Y. Zhang, F. Yu, Z. Ma, J. Li, J. Qian, X. Liang, and M. Zhang, Conductor temperature monitoring of high-voltage cables based on electromagnetic-thermal coupling temperature analysis, Energies, vol. 15, no. 2, p. 525, 2022.
[19] J. Lin and L. Cai, Research on the thermal aging life prediction of XLPE cable, Journal of Physics: Conference Series, vol. 1570, no. 1, p. 012050, 2020.
[20] M.A. Saleh, A.N. Alquennah, A. Ghrayeb, S.S. Refaat, H. Abu-Rub, and S.P. Khatri, A review on the lifetime estimation methods of XLPE power cables, IEEE Open Journal of Industry Applications, 2025.
[21] S. Ahmad, Z.H. Rizvi, and F. Wuttke, Unveiling soil thermal behavior under ultra-high voltage power cable operations, Scientific Reports, vol. 15, no. 1, p. 7315, 2025.
[22] P. Navarrete-Rajadel, P. Llovera-Segovia, V. Fuster-Roig, and A. Quijano-López, A sensor for multi-point temperature monitoring in underground power cables, Sensors, vol. 25, no. 17, p. 5490, 2025.
[23] D. Enescu, P. Colella, and A. Russo, Thermal assessment of power cables and impacts on cable current rating: An overview, Energies, vol. 13, no. 20, p. 5319, 2020.
[24] P.A. Wallace, D.M. Hepburn, C. Zhou, and M. Alsharif, Thermal response of a three core belted PILC cable under varying load conditions, 20th International Conference and Exhibition on Electricity Distribution-Part 1, June 2009, pp. 1–4.
[25] G.J. Anders, Rating of Electric Power Cables in Unfavorable Thermal Environment. Canada: John Wiley & Sons, 2005.
[26] IEC 60287-3-1:1995, Electric Cables Calculation of Current Rating - Part 3: Sections on Operating Conditions, International Electrotechnical Commission, 1995.
[27] BS IEC 60287-1-1:2006, Electric Cables Calculation of Current Rating - Part 1-1: Current Rating Equations (100% Loss Factor) and Calculation of Losses General, British Standards Institution, 2006.
[28] P. Zamani, A. Foomezhi, and S. G. Nohooji, "A review of medium voltage single-core cable armouring, induced currents and losses," *Energy and Power Engineering*, vol. 13, no. 7, pp. 272–292, 2021.
[29] D. Hepburn, C. Zhou, X. Song, G. Zhang, and M. Michel, Analysis of online power cable signals, International Conference on Condition Monitoring and Diagnosis, Beijing, China, Apr. 21–24, 2008, pp. 1175–1178.

